

# Electronic ballast of metal halide lamp for projector with digital control

**Abstract.** A novel digital control theory is proposed for the metal halide lamp electronic ballast used for the projector. The resonant ignition with  $LC_S C_P$  mode is adopted here, an adaptive digital control method for ignition is proposed to overcome the problem of the deviation for the passive components. A simple power closed loop method is proposed to make the lamp power constant without the power over shooting. In the laboratory, a 150W prototype is proposed to prove the rightness of the control theory.

**Streszczenie.** Zaproponowano zmodyfikowany układ obciążenia lampy halogenowej. Zastosowano zapłon rezonansowy oraz układ adaptacyjnego cyfrowego sterowania. Sprzężenie zwrotne zapewnia stały pobór mocy. Zbadano prototypowy projektor o mocy 150 W. (Układ elektroniczny z cyfrowym sterowaniem w projektorze z lampą halogenową)

**Keywords:** digital control, electronic ballast, power closed loop.

**Słowa kluczowe:** lampa halogenowa, projektor.

## Introduction

There are three lighting sources for the projector, which are the ultra high performance (UHP) lamp, the ultra high efficiency lamp (UHE) and the metal halide lamp. The UHP and UHE lamp are very expensive, and the replacement costs are very high. The metal halide lamp has low costs, and it is non-fragile as a line source. So here the metal halide lamp is chosen to be the lighting source for the low cost projector.

As one kind of the gas discharged lamp, the metal halide has negative resistance characteristics, so it must be used with ballast. The traditional magnetic ballast has very low power factor, big volume and high weight, so the high performance electronic ballast with high power factor, small volume and light weight becomes a trend [1-2]. The ballast studied in the paper is with digital control, and the microcontroller M908Q4ACE by FREESCALE is adopted to simplify the circuit and increase the power density of the system.

The half bridge is usually adopted in the ballast, and  $LC_S C_P$  resonant network is widely used because it does not need additional igniting circuit [3-5]. There are three passive

components in the  $LC_S C_P$  resonant network, and they all have deviation, which may make the ballast work unstable. This paper proposed a simple digital control method to make the ballast adapt the deviation of the passive components. Meanwhile, the digital control methods in the transition and steady stage are also proposed. The high frequency modulation method is adopted here to avoid the acoustic resonance problem.

## Configuration of the ballast

The block diagram of the ballast designed in this paper is shown in Fig 1. The circuit includes EMI filter, full-bridge rectifier, power-factor corrector, half-bridge inverter, load-resonant circuit, and interface circuit for microprocessor & drive circuit. A  $\pi$ -type EMI filter is used to satisfy EMC standards. A boost power-factor corrector is used to improve input power factor.  $LC_S C_P$  load-resonant circuit is used to realize lamp ignition and steady-state operation. An 8-bit microprocessor is used to control the lamp power and realize protection. Here MC33262 is chosen to control to PFC circuit, and the bus voltage is chosen to be 400V.

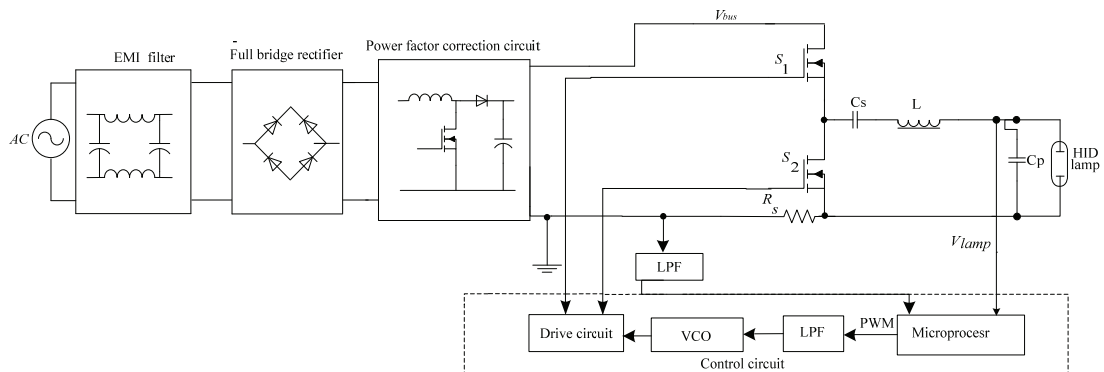


Fig. 1. Configuration of the ballast

## $LC_S C_P$ circuit analysis

From [6-7], the model of the high pressure discharged lamp can be expressed by its incremental impedance, as (1) shows.

$$(1) \quad z_L(s) = \frac{v_L(s)}{i_L(s)} = k \frac{s+z}{s+p}$$

Here  $z_L(s)$  is the incremental impedance of the lamp,  $v_L(s)$  is the lamp voltage perturbation and  $i_L(s)$  is the lamp current perturbation.  $Z$  is a negative real value and  $k$  is a positive real value. Then the incremental impedance of the lamp in the high working frequency can be described as follows.

$$(2) \quad R_\infty = z_L(\infty) = k$$

$R_{\infty}$  is a positive real value, so the incremental lamp voltage and current will be proportional. Here a 150W metal halide lamp produced by fushan lighting company is adopted, the acoustic resonance phenomena does not happen when the working frequency is higher than 150kHz, but high frequency modulation method is also adopted to avoid the acoustic resonance. The equivalent circuit of half-bridge  $LC_S C_P$  resonance inverter can be seen as follows.

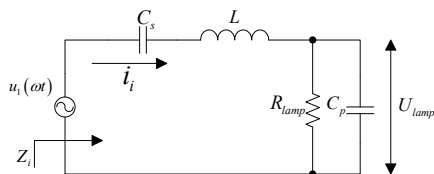


Fig. 2. Equivalent circuit of half-bridge  $LC_S C_P$  resonance inverter

From paper[8], a sine waveform based on frequency control  $x(t)$  can be described as a complicated vector form.

$$(3) \quad x(t) = \text{Re}[x(t)e^{j\int\omega_s(t)dt}]$$

Here  $\omega_s(t)$  is the instantaneous angular frequency of the variable. So the small signal of the  $LC_S C_P$  can be described as follows.

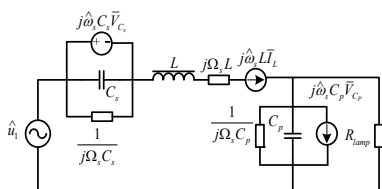


Fig. 3. Small signal model of  $LC_S C_P$  circuit

### Digital control method for the ignition

$LC_S C_P$  circuit can not only provide ignition voltage of the lamp, but also can provide the lamp voltage in steady state without additional circuit. In practical use, the value of  $C_S$  is far larger than the value of  $C_P$ , so  $C_P$  has main working function in the ignition stage, and  $C_S$  has main working function in the steady state. Table .1 shows the characteristic parameters for the  $LC_S C_P$  converter.

Table.1 Parameters of  $LC_S C_P$  inverter

	frequency	impedance	quality factor
series resonance	$\omega_s = 1/\sqrt{LC_s}$	$Z_s = \omega_s L$	$Q_s = \frac{Z_s}{R_{lamp}}$
parallel resonance	$\omega_p = 1/\sqrt{LC_p}$	$Z_p = \omega_p L$	$Q_p = \frac{R_{lamp}}{Z_p}$

The voltage-transfer characteristic of the  $LC_S C_P$  circuit can be calculated as follows.

(4)

$$|H_v(j\omega)| = \frac{U_{lamp}}{U_1} = \frac{1}{\sqrt{\left[1 - \left(\frac{\omega}{\omega_s}\right)^2 - 1\right]^2 \left(\frac{C_p}{C_s}\right)^2 + Q_s^2 \left[\frac{\omega}{\omega_s} - \frac{\omega_s}{\omega}\right]^2}}$$

Fig. 4 shows the voltage-transfer characteristic of the  $LC_S C_P$  circuit. The traditional sweeping frequency method is to set the initial frequency (1) point and the critical frequency (2) point, then change the working frequency from (1) point to (2) point, and if the lamp is on on (3) point, the system will work in the left resonant cavity because the impedance of the lamp decreases rapidly after the lamp is

ignited. The frequency (4) point is set after the lamp is on to make the lamp have a initial lamp current to maintain gas ionization in the lamp.

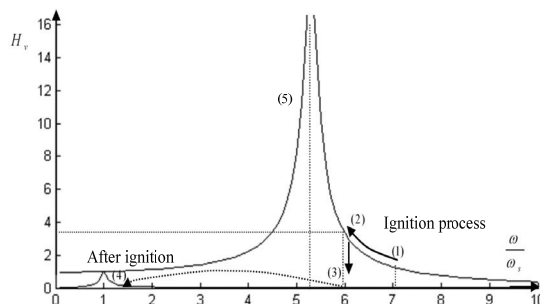


Fig. 4.  $LC_S C_P$  circuit voltage gain

The traditional method ignores the deviations of the passive components, the inductor value usually has 10% deviation and the capacitor value usually has 20% deviation. Though we can buy the components with little deviation, their costs is much higher. With traditional igniting method, two things may happen, one is that the critical frequency is too high to ignite the lamp, and the other is that the initial frequency is so low that the inrush current in the resonant cavity is very high, which may break the ballast, and the worst situation is that the initial frequency is the resonant frequency.

In the paper, the influence of the deviations for the components in the  $LC_S C_P$  circuit can be described by their sensitivities for the voltage gain  $H_v$ . The unite sensitivity is defined as follows.

$$(5) \quad S_x^{H_v} \Big|_{x=x_N} = \frac{\partial H_v}{\partial x} \cdot \frac{x_N}{H_v(x_N)}$$

If the sensitivity is negative,  $H_v$  decreases with the increasing of the parameter, and if the sensitivity is positive,  $H_v$  increases with the increasing of the parameter.

Here we define that  $k = \omega/\omega_p$ , then the sensitivities for  $C_P$ ,  $C_S$ ,  $L$  can be described as follows.

(6)

$$S_{C_s}^{H_v} = \frac{\frac{C_p}{C_s} \left[ 1 - (k^2 - 1) \frac{C_p}{C_s} \right] (k^2 - 1)}{\left[ 1 - (k^2 - 1) \frac{C_p}{C_s} \right]^2 + Q_s^2 \left( k - \frac{1}{k} \right)^2}$$

$$S_{C_p}^{H_v} = \frac{\left( 1 - (k^2 - 1) \frac{C_p}{C_s} \right) \frac{C_p}{C_s} + 2Q_s^2 \left( 1 - \frac{1}{k^2} \right)}{\left[ 1 - (k^2 - 1) \frac{C_p}{C_s} \right]^2 + Q_s^2 \left( k - \frac{1}{k} \right)^2}$$

$$S_L^{H_v} = \frac{k^2 \frac{C_p}{C_s} \left( 1 - (k^2 - 1) \frac{C_p}{C_s} \right) - Q_s^2 \left( \frac{3}{2} k^2 + \frac{1}{2k^2} + 2 \right)}{\left[ 1 - (k^2 - 1) \frac{C_p}{C_s} \right]^2 + Q_s^2 \left( k - \frac{1}{k} \right)^2}$$

The typical value for  $C_S$  is about 1uF, and the value of  $C_P$  must be small enough to ignite the lamp, and its typical value is several nano farads. So we get that  $S_{C_s}^{H_v} \ll S_{C_p}^{H_v} \approx S_L^{H_v}$ , which means that  $C_p$  and  $C_L$  have main influence for the  $LC_S C_P$  circuit, and the influence of  $C_S$  can be ignored in igniting state.

To lower the influence for the system by the deviations of the passive components, the critical frequency is set to (5) point which is lower than the resonant frequency, and the highest voltage in the igniting stage is limited. In the practical use, we can increase the initial frequency, decrease the

critical frequency which is lower than the resonant frequency, and limit the highest voltage in the igniting stage, then the igniting control method can not only adapt the deviations of the passive components, but also can adapt the old lamp. The program flow diagram is shown in fig.5(a), and fig.5(b) shows the sweeping diagram,  $f_2$  is the critical frequency without deviations of the passive components, and the left and right sides of the resonant cavities shows the maximum variation of passive components to the  $LCsCp$  circuit. It's evident that no matter how the values of the passive components change, the  $LCsCp$  circuit can get the igniting voltage which is high enough to ignite the lamp because of the existence of the limitation for the lamp voltage. The sweeping frequency varies from  $f_3-f_0$  to  $f_1-f_0$ .

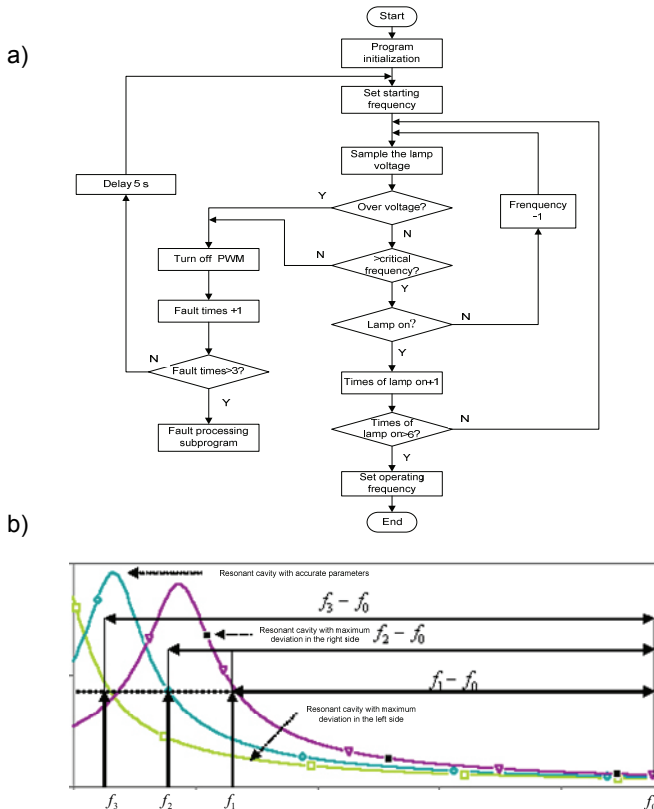


Fig. 5. Flow chart and sweeping diagram in ignition stage

### Digital control methods in transition and steady state

In the transition stage, if we adjust the lamp power too fast, the lamp power may overshoot, and the  $di/dt$  and  $du/dt$  are also very high, so constant frequency control is adopted here, the lamp power increases steadily as the lamp impedance increase until the lamp power reaches its rated power.

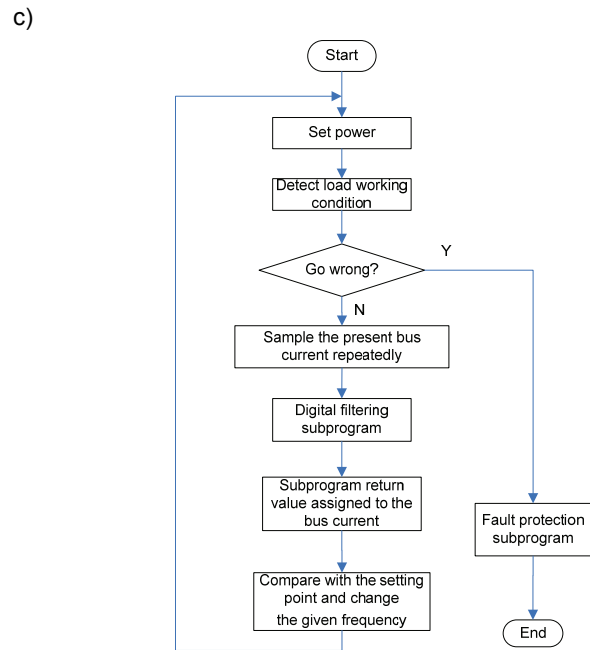
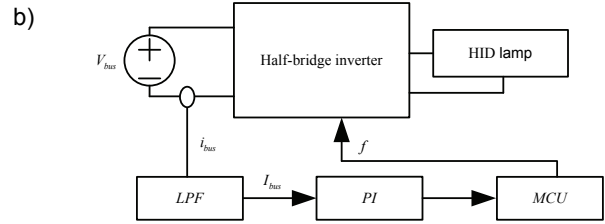
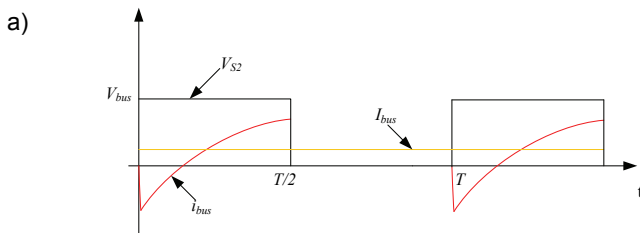


Fig. 6. (a) The waveforms of the bus current (b) Diagram of power control loop (c) The control flow chart in steady state

The bus current waveform in steady state of  $LCsCp$  circuit is shown in fig.6(a). The bus voltage can be described as follows.

$$(9) \quad i_{bus} = \frac{1}{2\pi} \int_0^{2\pi} i_{bus} d\theta + \sum_1^{\infty} \sqrt{a_n^2 + b_n^2} \sin(n\theta + \tan^{-1} \left[ \frac{a_n}{b_n} \right])$$

$$\text{Here: } a_n = \frac{1}{\pi} \int_0^{2\pi} i_{bus} \cos(n\theta) d\theta; \quad b_n = \frac{1}{\pi} \int_0^{2\pi} i_{bus} \sin(n\theta) d\theta;$$

The average input power can be calculated in (10).

$$(10) \quad P_{in-av} = \frac{1}{2\pi} \int_0^{2\pi} V_{bus} i_{bus} d\theta$$

Then the equation (11) can be gotten.

$$(11) \quad P_{in-av} = V_{bus} \times \frac{1}{2\pi} \int_0^{2\pi} i_{bus} d\theta = V_{bus} I_{bus}$$

In the steady state, the relationship between the lamp power  $P_{lamp}$  and the average input power  $P_{in-av}$  is shown in

$$(12) \quad P_{lamp} = \eta \cdot P_{in-av} = \eta \cdot V_{bus} I_{bus}$$

$\eta$ : the efficiency of the converter.

Here,  $V_{bus}$  is the output voltage of the boost PFC circuit and it is almost constant. The lamp power control can be transformed to control  $I_{bus}$ . In Fig.1  $I_{bus}$  is detected by  $R_s$  and  $I_{bus}$  is obtained through a low-pass filter. The microprocessor detects and controls it to the expected value. Therefore, the closed-loop control of the lamp power is realized. To avoid the acoustic resonance, the high

frequency modulation method is adopted here, the working frequency varies around the center frequency. So the high frequency energy has a certain frequency band, not a single frequency point, which avoids the acoustic resonance.

Fig.6(b) shows the diagram of power control loop and fig.6(c) shows the control flow chart in steady state. Here we sample the bus voltage several time and the average value is used to do the power closed loop. Open-circuit, hot-lamp and short-circuit protection is designed to protect the electronic ballast.

Ignition failure can be detected as the electronic ballast is in open-circuit or hot lamp state, while  $I_{bus}$  is small. The ballast attempts to ignite the lamp for three times, which interval is 10 minutes. If the lamp is in hot-lamp state, it can be cooled down during the interval and can be ignited normally. If the lamp is in open-circuit state, it can not be ignited during the intervals. The microprocessor stops the output of the ballast. Moreover, Short-circuit protection can be detected by the lamp voltage  $V_{lamp}$ . If the lamp is in short-circuit state,  $V_{lamp}$  is zero.

### Experimental results

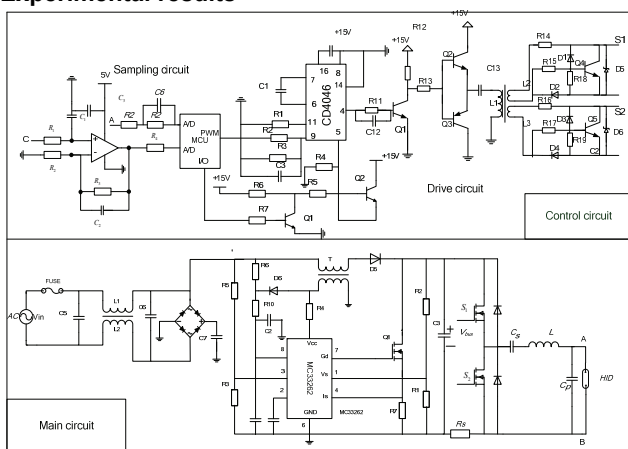


Fig. 7. The control circuit of the system

Fig.7 shows the schematic of the system, including the main circuit and the control circuit. The control circuit is made of the sampling circuit and the drive circuit, here the chip CD4046 is used to realize voltage control oscillator (VCO) function. The PWM signal from the MCU is changed to a DC signal, then the DC signal is changed to a frequency signal through VCO circuit to drive the half bridge circuit.

In the system, the working frequency is chosen to be 166kHz, and value of  $C_s/C_p$  is usually larger than 100, here it's chosen to be 400. and the value of  $C_p$  is usually verysmall, here it's chosen to be 1.65nF, then the value of  $C_s$  can be calculated. Through the test, the lamp current is about 1.6A, and the lamp voltage is about 110V, then the value of the inductor can be gotten from (4).The final parameters are as follows:  $C_s = 680$  nF,  $C_p = 1.65$  nF,  $L = 90$   $\mu$ H. The resonant frequency is 130kHz, the initial frequency and the critical frequency are chosen be 180kHz and 110kHz. Since the break down voltage of the lamp used here is about 1500V, the limiting value of the lamp voltage is chosen to be 2000V.

Fig.8(a) is the frequency sweeping waveforms without deviation, and fig.8(b) is the frequency sweeping waveforms with 20% deviation of the value for  $C_p$ , so it can be seen from the figures that the lamp can be ignited successfully, and the only different is the frequency sweeping time. In the experiment, 20 prototypes are made, and the value of the inductor is with 10% deviation, the value of the capacitor is

with 20% deviation, and all the prototypes can ignite the lamp steadily. Fig.8(c) is the sampling signal of the lamp voltage in the open-circuit state, and fig.8(d) is the sampling signal of the bus current in the short-circuit stage, then the ballast can stop working when the ballast is in the wrong working condition, which protect the ballast very well. Fig.8 (e) shows the test waveforms of the lamp current and voltage, and fig8 (f) shows the dynamic v-i characteristic of the lamp.

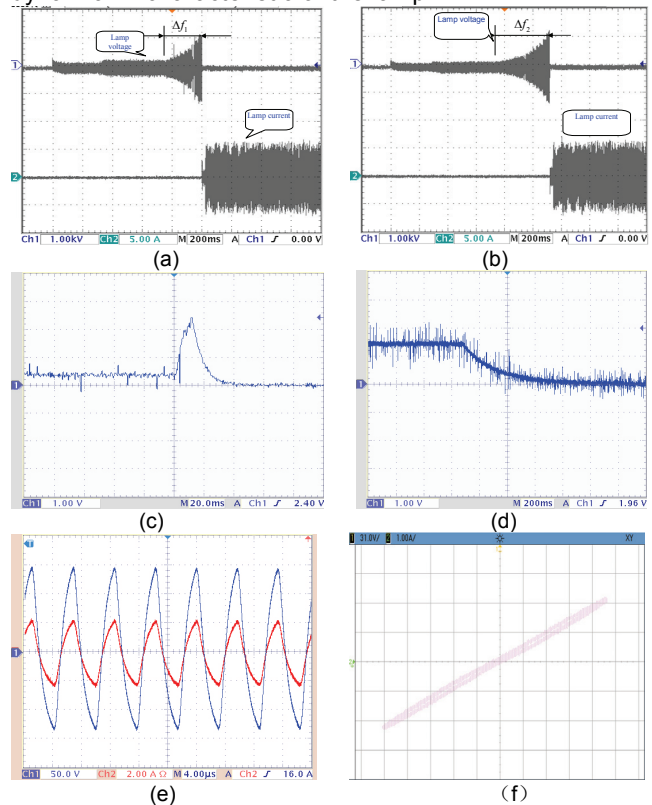


Fig. 8. The test results in the experiment

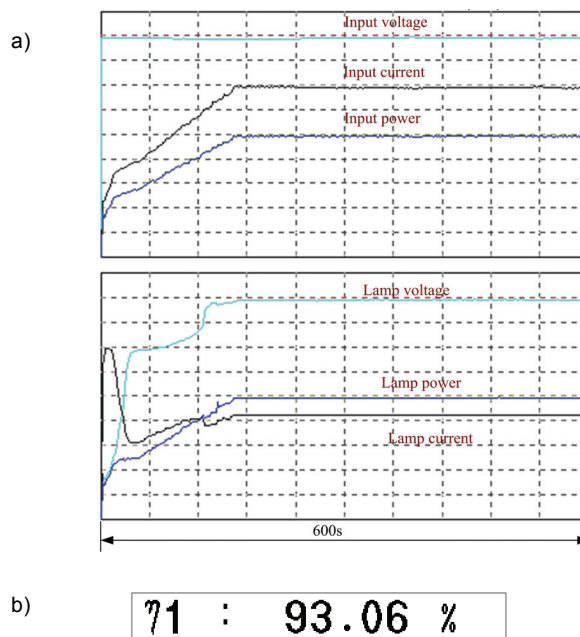


Fig. 9. The test results of the system

Fig.9 (a) shows the test results of input and output side for the ballast by UI2000 electronic ballast tester, and

it's evident that the input and the output power all increase steadily in the transition stage, which proves the control theory, and when the lamp power is constant in the steady state, which proves the rightness of the power-closed loop control method. Fig 9(b) shows the efficiency of the electronic ballast tested by HIOKI 3193 POWER HITESTER, and it's as high as 93.06%. Fig.10 shows the prototype of the ballast and the projector.

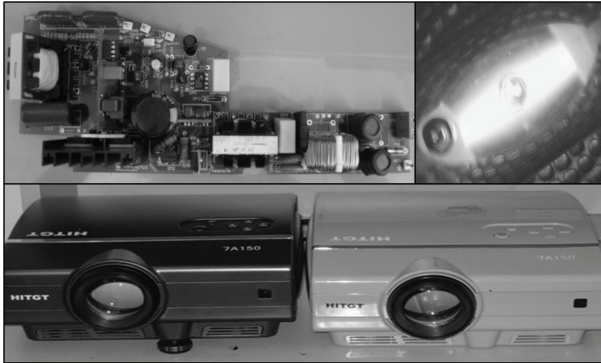


Fig. 10. The prototype used in the laboratory

### Conclusion

A digital control method is proposed in the paper for the metal halide lamp electronic ballast used in the projector. A reliable ignition method is proposed considering the deviation of the components in the  $LC_S C_P$  circuit. The control methods are also presented for the lamp in the transient state, the steady state and the wrong working condition. The experiment results show that the system can be ignited reliably, transit smoothly and the lamp power can be kept constant accurately, and the electronic ballast can be protected rapidly when the system is in the open circuit and short circuit state.

*This work is supported by the Scientific and Technological Project of Heilongjiang Province under Grant GB02A105.*

### REFERENCES

- [1] Francisco J. Azcondo, F. Javier Díaz, Christian Brañas, Microcontroller Power Mode Stabilized Power Factor Correction Stage for High Intensity Discharge Lamp Electronic Ballast, *IEEE Trans. Power Electron.*, 22 (2007), No. 3, 845-853
- [2] Huang-Jen Chiu, Hsiu-Ming Huang, Yu-Kang Lo, Chia-Hsing Li, High-Frequency Dimmable Electronic Ballast for HID Lamps, *IEEE Trans. Power Electron.*, 21 (2006), No. 5, 1452-1458
- [3] Tsai-Fu Wu, Te-Hung Yu, Analysis and Design of a High Power Factor, Single-Stage Electronic Dimming Ballast, *IEEE Trans. Ind. Appl.*, 21 (2006), No. 5, 1452-1458
- [4] J. Marcos Alonso, Cecilio Blanco, Emilio L'opez, Analysis, Design, and Optimization of the LCC Resonant Inverter as a High-Intensity Discharge Lamp Ballast, *IEEE Trans. Power Electron.*, 13 (1998), No. 3, 573-585
- [5] Jesús Cardesín, José Marcos Alonso, Emilio López-Corominas, Design Optimization of the LCC Parallel-Series Inverter With Resonant Current Mode Control for 250-W HPS Lamp Ballast, *IEEE Trans. Power Electron.*, 20 (2005), No. 5, 1197-1204
- [6] E. Deng, S. Cuk., Negative incremental impedance and stability of fluorescent lamps, *IEEE Applied Power Electronics Conference and Exposition*, 2 (1997), 1050-1056
- [7] M. A. Dalla Costa, J. M. Alonso, J. García-García, Analysis, Design and Experimentation of a Closed-Loop Metal Halide Lamp Electronic Ballast, *IEEE Industry Applications Conference*, 3 (2006), 1384-1390
- [8] Yan Yin, Regan Zane, John Glaser, Small-Signal Analysis of Frequency-Controlled Electronic Ballasts, *IEEE transactions on circuits and systems—1*, 50 (2003), No. 8, 1103-1110

**Authors:** dr. Yijie Wang, Harbin Institute of Technology, China, E-mail: [wangyijie1982@gmail.com](mailto:wangyijie1982@gmail.com); prof. Wei Wang, Harbin Institute of Technology, China, E-mail: [wangwei602@hit.edu.cn](mailto:wangwei602@hit.edu.cn); prof. Dianguo Xu, Harbin Institute of Technology, China, [xudiang@hit.edu.cn](mailto:xudiang@hit.edu.cn)  
**Correspond author:** E-mail: [wangyijie1982@gmail.com](mailto:wangyijie1982@gmail.com)